ELSEVIER

Biophysical Chemistry 119 (2006) 158 – 169

Biophysical Chemistry

http://www.elsevier.com/locate/biophyschem

The structure of human apolipoprotein E2, E3 and E4 in solution 1. Tertiary and quaternary structure

Anne Barbier [a,b], Vanessa Clément-Collin [b], Alexander D. Dergunov [c,*], Athanase Visvikis [a], Gérard Siest [a], Lawrence P. Aggerbeck [b]

[a] *Centre du Médicament, Université Henri Poincaré Nancy 1, 30 rue Lionnois, 54000 Nancy, France*
[b] *Centre de Génétique Moléculaire UPR 2167, Centre National de la Recherche Scientifique, Avenue de la Terrasse, 91198 Gif-sur-Yvette, Associé à l'Université Pierre et Marie Curie (Paris VI), France*
[c] *National Research Centre for Preventive Medicine, 10 Petroverigsky street, 101953 Moscow, Russia*

Received 14 March 2005; received in revised form 20 July 2005; accepted 21 July 2005
Available online 2 September 2005

Abstract

Three recombinant apoE isoforms fused with an amino-terminal extension of 43 amino acids were produced in a heterologous expression system in *E. coli*. Their state of association in aqueous phase was analyzed by size-exclusion liquid chromatography, sedimentation velocity and sedimentation equilibrium experiments. By liquid chromatography, all three isoforms consisted of three major species with Stokes radii of 4.0, 5.0 and 6.6 nm. Sedimentation velocity confirmed the presence of monomers, dimers and tetramers as major species of each isoform. The association schemes established by sedimentation equilibrium experiments corresponded to monomer–dimer–tetramer–octamer for apoE2, monomer–dimer–tetramer for apoE3 and monomer–dimer–tetramer–octamer for apoE4. Each of the three isoforms exhibits a distinct self-association pattern. The apolipoprotein multi-domain structure was mapped by limited proteolysis with trypsin, chymotrypsin, elastase, subtilisin and *Staphylococcus aureus* V8 protease. All five enzymes produced stable intermediates during the degradation of the three apoE isoforms, as described for plasma apoE3. The recombinant apoE isoforms, thus, consist of N- and C-terminal domains. The presence of the fusion peptide did not appear to alter the apolipoprotein tertiary organization. However, a 30 kDa amino-terminal fragment appeared during the degradation of the recombinant apoE isoforms resulting from cleavage in the 273–278 region. This region, not accessible in plasma apoE3, results from a different conformation of the C-terminal domain in the recombinant isoforms. A specific pattern for the apoE4 C-terminal domain was observed during the proteolysis. The region 230–260 in apoE4, in contrast to that of apoE3 and apoE2, was not accessible to proteases, probably due to the existence of a longer helix in this region of apoE4 stabilized by an interdomain interaction.

Keywords: Apolipoprotein E; Receptor-binding domain; Protein conformation; Lipid–protein interactions; Lipoprotein

1. Introduction

The 34.2 kDa apolipoprotein E (apoE) is a key participant in cholesterol metabolism and transport both in plasma and brain due to its interaction with several receptors, the most common being the LDL-receptor [1] and the LDL-receptor-related protein [2]. ApoE possesses a genetic polymorphism due to a single arginine–cysteine interchange. Three common isoforms, apoE2, apoE3 and apoE4, are the products of three alleles of the APOE gene. ApoE2 (Cys112, Cys158) displays defective receptor binding and is associated with type III dyslipidemia [3,4]. ApoE3 (Cys112, Arg158) is the most common isoform, whereas apoE4 (Arg112, Arg158) has been associated with late-onset Alzheimer's disease [5]. The three apoE isoforms differ drastically in their distribution among lipoproteins, in

Abbreviations: apoE, apolipoprotein E; CT domain, carboxyl-terminal domain; DTT, dithiothreitol; LDL, low-density lipoprotein; NT domain, amino-terminal domain; R_S, Stokes radius; V_e, elution volume.

* Corresponding author. Tel.: +7 95 927 0324; fax: +7 95 928 5063.
E-mail address: dergunov@img.ras.ru (A.D. Dergunov).

0301-4622/$ - see front matter © 2005 Elsevier B.V. All rights reserved.
doi:10.1016/j.bpc.2005.07.010

their binding to β-amyloid peptide [6–8] and in their influence on neuronal growth and regeneration [9].

Plasma apoE3 is composed of two domains with different stabilities to denaturant [10,11] that are linked via a protease-sensitive loop. The 22 kDa amino-terminal domain (NT domain, residues 1–191) contains the LDL receptor-binding site [12–17] and the heparin-binding site [18] and has weak lipid-binding capability [4]; the 10 kDa carboxyl-terminal domain (CT domain, residues 210–299) accommodates high-affinity lipid-binding sites and apoE self-association sites [10,11,19]. Crystallographic structures of the NT domains of the three apoE isoforms have been obtained and modeled by a four-helix bundle of amphipathic α-helices [20], the most significant differences appearing to be confined to helix 3 of apoE2. In comparison to apoE3, the apoE4 NT domain has an additional salt bridge between Arg112 and Glu109, causing a displacement of the Arg61 side chain [21]. Studies of recombinant mutants have provided evidence of a domain interaction [22]. The free energy of stabilization of the apoE NT domain is approximately 10 kcal/mol, similar to that of globular proteins. A recent study has demonstrated that the NT domains of the three isoforms [23] as well as the intact isoforms [24] have different stabilities to Gdn–HCl- and temperature-induced denaturation. The presence of a partially folded intermediate for NT domain of apoE4 unfolding has been suggested [23].

Unlike the NT domain, the structure of the CT domain of apoE is unknown although a proteolytic fragment comprising residues 223–272 has been crystallized [25]. It bears a lower free energy of stabilization, comparable to properties of other apolipoproteins [11]. Residues 267–299 are responsible for apoE self-association, while residues 245–266 determine lipoprotein-binding preferences [10,18,19,26]. Both plasma apoE3 [10] and an apoE of unspecified phenotype [19] associate in aqueous phase primarily as tetramers and, more recently, a monomer–tetramer–multimer equilibria has been suggested [27,28]. There is only one comparative study on the association of two recombinant apolipoprotein isoforms in a lipid-free environment. ApoE3 and apoE4 existed as slow-equilibrium mixtures of monomers, tetramers, and octamers, with a small proportion of higher oligomers. ApoE4 had a greater propensity to self-associate [29]. Also, the N-terminal-truncated apoE4 (72–299) showed a wider and more complicated species distribution compared to apoE3 (72–299) [30]. Two different models describe apoE tetramerization mediated by the CT domain, a four-helix bundle [10] and a dimer of dimers [31].

The use of three recombinant apoE isoforms allowed us to compare for the first time the association schemes for all three apolipoproteins in aqueous solution by performing size exclusion gel chromatography, sedimentation velocity and sedimentation equilibrium experiments. Secondly, a study of the domain structure of the three apoE isoforms by limited proteolysis confirmed a two-domain organization of all the proteins and revealed some peculiarities in apoE4 tertiary structure. In an accompanying paper, the relationship of the secondary and tertiary structure to the stability of the three isoforms to chemical denaturation and temperature is described. Together, these data underline the structural peculiarities that result in different functions of these apoE isoforms.

2. Materials and methods

2.1. Preparation of apoE

Human plasma apoE3 was prepared as described previously [32]. The three recombinant apoE isoforms were prepared as described previously [33,34]. The proteins were expressed with a fused peptide of 43 amino acids, which carries a polyhistidine cluster used for metal chelating affinity chromatography. The fusion peptide was not cleaved and the molecular masses of the recombinant apoE isoforms were 39 kDa. The purification was carried out under denaturing conditions in a single step by a decrease of pH. The purified proteins were lyophilized and stored at a concentration of 1 mg/ml in 100 mM NH_4HCO_3. The purity of the proteins was evaluated by SDS-PAGE and mass spectrometry. To eliminate aggregates that may accumulate during storage of apolipoprotein solution, the apoE before use was denatured in 6 M guanidine hydrochloride, 10 mM Tris–HCl pH 8.0, 1 mM EDTA, 2% β-mercaptoethanol by incubation overnight at 4 °C. The apolipoprotein solutions were then dialyzed extensively against 100 mM NH_4HCO_3, mM β-mercaptoethanol. Protein concentrations were determined by measuring the absorbance at 280 nm in the presence of 6 M guanidine hydrochloride, 2% β-mercaptoethanol [35] and with the Protein Assay ESL kit (Boehringer Mannheim, Mannheim, Germany).

2.2. Gel permeation chromatography

The experiments were carried out with a column (1 × 30 cm) of Superose 12 (Pharmacia Biotech, Upsalla, Sweden) equilibrated with 100 mM NH_4HCO_3, 1 mM β-mercaptoethanol at a flow rate of 0.5 ml/min at 4 °C. The column was calibrated with proteins of known Stokes radii R_S [36]. The total volume, V_t, and the exclusion volume, V_0, of the column were determined with $NaNO_3$ and Blue Dextran, respectively. A calibration curve was constructed as described by Uversky [37] and gave the following relationship:

$$\frac{1000}{V_e} = 0.615 \cdot R_S + 58.66 \quad (1)$$

The diffusion coefficients, D, were estimated from protein R_S values by Eq. (2):

$$D = \frac{kT}{6\pi \cdot \eta \cdot R_S} \quad (2)$$

where k is the Boltzmann constant ($1.38 \cdot 10^{-16}$ erg deg^{-1}), T is the experimental temperature (293.2 K) and η is the solvent viscosity (1.015 cP) at a temperature T. The experiments were performed 3 times and they were entirely reproducible.

2.3. Analytical ultracentrifugation

Sedimentation velocity and sedimentation equilibrium experiments were performed in a Beckman Optima XL-A analytical ultracentrifuge at 4 °C in 100 mM NH_4HCO_3, 1 mM β-mercaptoethanol using an An-60 Ti rotor and XL-A Data Analysis Software. Protein concentrations were 0.35 mg/ml for apoE2 and apoE3 and 0.25 mg/ml for apoE4. Sedimentation velocity experiments were performed twice at 60,000 rpm for 3 h. Scans through the cell were recorded every 6 min providing time-dependent profiles of the change in the absorbance at 280 nm. The values for the sedimentation coefficients, s, and the number of components were determined by a time derivative of the concentration profile to calculate the apparent sedimentation coefficient profile, $g(s^*)$ [38], and the accuracy was verified by the residuals. A technique of modeling of the $g(s^*)$ distribution with Gaussians to obtain a molar mass estimate has been used also by Philo [39] and it has been argued [40] that the results from the $g(s^*)$ modeling are conceptually similar to more complex analysis that deconvolutes diffusion effects [41]. The apparent s values were corrected for the temperature and solvent to standard conditions with Eq. (3):

$$s_{20,w} = s_{obs} \cdot \frac{\eta_{T,w} \cdot \eta_s \cdot (1 - \overline{v} \cdot \rho_{20,w})}{\eta_{20,w} \cdot \eta_w \cdot (1 - \overline{v} \cdot \rho_{T,s})} \quad (3)$$

where s_{obs} is the observed sedimentation coefficient in a particular solvent and temperature, $\eta_{T,w}$ (1.567 cP) and $\eta_{20,w}$ (1.002 cP) were the water viscosities at the experimental temperature T (4 °C) and at 20 °C, respectively, η_s and η_w were the viscosity of the solvent and water at a standard temperature (η_s/η_w=1.013 at 20 °C), $\rho_{20,w}$ is the density of water at 20 °C (0.998234 g/l) and $\rho_{T,s}$ is that of the solvent at 4 °C (1.00272 g/l), $\bar{v}$ is the partial specific volume of apoE calculated from its amino acid composition (SEDNTERP program by John Philo) for a particular temperature (0.720 ml/g at 4 °C and 0.726 ml/g at 20 °C). Diffusion coefficients were calculated from the sedimentation velocity data using the SVEDBERG program by John Philo (http://www.jphilo.mailway.com). The values of the diffusion and sedimentation coefficients permit an estimation of the molecular mass of each species in solution using Eq. (4):

$$MM = \frac{RT \cdot s}{D \cdot (1 - \overline{v} \cdot \rho)}. \quad (4)$$

Sedimentation equilibrium experiments for each isoform were performed once at three different speeds 8000, 10000 and 14000 rpm, each for 24 h. As a last step, centrifugation at 42,000 rpm was performed for 3 h. Scans at 280 nm were recorded along the cell each 2 h until there were no further changes in the scans and the data were analyzed under equilibrium conditions. The base line, corresponding to the absorption of the buffer without protein, was subtracted. The profiles were analyzed with Beckman XL-A Data Analysis, XL-A UltraScan (Borries Demeler) and custom

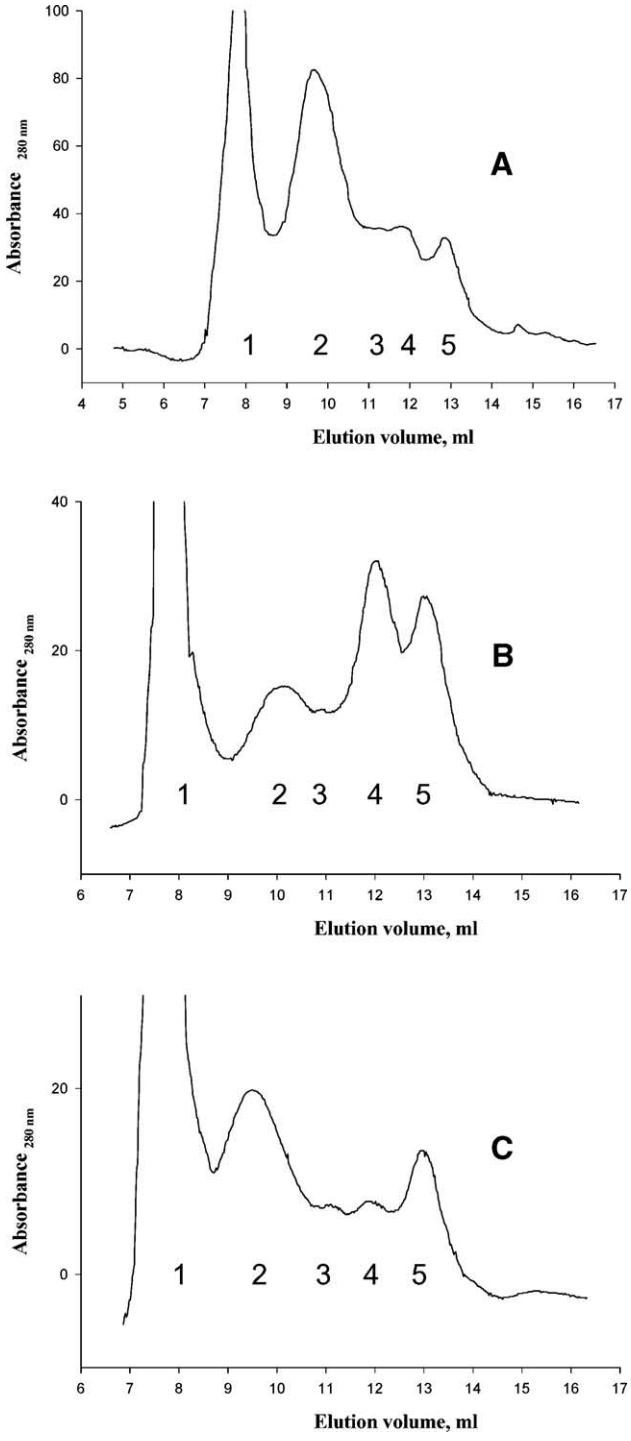

Fig. 1. Elution profiles of the three recombinant apoE isoforms upon gel filtration on a Superose 12 column. The column was equilibrated with 100 mM NH_4HCO_3 and 1 mM β-mercaptoethanol at 4 °C with a flow rate of 0.5 ml/min. 20 μg of each apoE isoform at a concentration 1 mg/ml were loaded on the gel. (A) ApoE2, (B) apoE3, and (C) apoE4.

written software, which provided an association model for the apolipoproteins. Representative results are shown but the interpretations were similar in all cases.

2.4. Proteolysis experiments

Proteolytic enzymes were frozen in water solution at −80 °C. Proteolyses were performed as previously described [11] and they have been reproduced at least 3 times for each isoform. The three apoE isoforms were diluted in 100 mM NH_4HCO_3, 1 mM β-mercaptoethanol to a concentration of 0.2 mg/ml. The time course of hydrolysis was followed by incubation of the apolipoprotein with the various proteolytic enzymes at different concentrations at room temperature. At each time point an aliquot of the reaction mixture was adjusted to 1 mM phenylmethanesulfonyl fluoride to inhibit the protease (trypsin, chymotrypsin, elastase and subtilisin) and then frozen in dry ice and stored at −20 °C until analysis, except in the case of *S. aureus* V8, where the reaction was terminated by freezing in liquid nitrogen followed by immediate analysis. The reaction products were separated by SDS-PAGE on a 15–20% gradient polyacrylamide gel adapted from the Laemmli method, but substituting 2-amino-2-methyl-l,3-propanediol for Tris. The protein bands were stained with Coomassie Blue R-250. Immunoblotting was performed with three mouse anti-apoE monoclonal antibodies 3B7, 1D7 and 3H1 characterized previously [18,42]. These antibodies were the gift of Drs. R. Milne and Y. Marcel of the Hearth Institute, University of Ottawa, Canada. The second anti-mouse antibody used was from Pierce (Rockford, IL, USA).

3. Results

3.1. Gel filtration study

In 100 mM NH4HCO3, 1 mM β-mercaptoethanol, the three recombinant apolipoprotein E isoforms (apoE2, E3 and E4) separated into at least five species; the representative profiles are given in Fig. 1. The first peak (with an elution volume of 8 ml) eluted in the void volume and was composed of a small amount of protein aggregates that extensively scattered light. The second peak, which was the major protein-containing peak representing up to 65% of the soluble species in apoE2 and apoE4, had an elution volume of 9.5– 10 ml corresponding to the R_S values of 6.6–7.7 nm (Table 1). The two following peaks, with elution volumes of 11–12 ml, contained species with R_S values of approximately 5.0 and 4.0 nm, respectively. These species were minor components in apoE2 and apoE4 solutions while a component with an R_S of approximately 4.0 nm represented 50% of the soluble protein in apoE3 solutions. The last peak with an elution volume of 13 ml, which was relatively abundant, did not contain any protein following analysis by SDS-PAGE (data not shown). In comparison, solutions of human plasma apoE3 at a concentration of 0.5 mg/ml contained mainly tetramers [10,19] with a Stokes radius at 6.6 nm. Thus, the species with R_S values of 6.6–7.7 nm corresponded to apoE tetramers whereas the species with R_S values of 4.7–5.2 and 4.0–4.1 nm represented structures that were less self-associated. Gel filtration of the three recombinant proteins and human plasma apoE3 on a TSK3000SW column at 20 °C gave similar results to those obtained at 4 °C (data not shown). Based on the R_S values, the diffusion coefficients $D_{20,w}$ were calculated for these structures (Table 1). The estimation of the D value from R_S has been found to be quite reasonable in a previous study of apoE3 [10].

From the standard curve for globular proteins, the R_S value of 6.6 nm would correspond to a molecular mass of 300 kDa, much larger than that of the plasma apoE tetramer, i.e. 136 kDa measured by other independent approaches [10]. The elongated shape of apoE seems to be responsible for this discrepancy, apoE being characterized by a frictional ratio f/f_0 of 1.79 [10]. To define more precisely the association state of three apoE isoforms in solution, their behavior was analyzed by analytical ultracentrifugation.

3.2. Sedimentation velocity experiments

The shape of the boundary between protein-free and protein-containing zones was dependent on the time of

Table 1
Hydrodynamic properties and molecular masses of three recombinant apoE isoforms in aqueous solution

	apoE2			apoE3			apoE4		
	1	2	3	1	2	3	1	2	3
R_S, nm	7.31	4.74	4.10	6.64	4.98	4.05	7.67	5.20	3.96
$s_{20,w}$, S	5.65	3.68	2.64	5.61	3.35	1.96	5.51	3.80	2.87
$D_{20,w}$, 10^{-7} cm^2 s^{-1} (a)	3.08	4.03	5.23	3.03	4.08	5.10	3.00	4.24	5.22
$D_{20,w}$, 10^{-7} cm^2 s^{-1} (b)	2.93	4.51	5.22	3.22	4.30	5.28	2.79	4.11	5.40
MM, Da	171,100	91,800	44,900	153,500	69,300	32,400	175,800	81,900	47,600

The data are given for three major structures in the solution of each protein. Stokes radii R_S were determined by size exclusion chromatography on a Superose 12 column. Diffusion coefficients $D_{20,w}$ were determined from the sedimentation velocity data (a) or were calculated from R_S values (b) by Eq. (2). Sedimentation coefficients $s_{20,w}$ were determined from the analysis of the distribution of the sedimentation coefficients, obtained from profiles in sedimentation velocity experiments. Molecular masses were estimated by Eq. (4).

centrifugation (Fig. 2). The presence of the different species can be qualitatively verified: a slowly sedimenting part of the boundary observed at absorbances below 0.3, a rapidly spreading heterogeneous boundary between 0.3 and 0.6, and a strong depletion of the solution plateau indicating larger species. The time derivative method $g(s^*)$ was applied to analyze the sedimentation velocity data (Fig. 3), in which six components were demonstrated after deconvolution. Analogously, Perugini et al. [29] observed five species for apoE3 and apoE4 by continuous size distribution analysis. Each apoE isoform included one major species with a sedimentation coefficient, $s_{20,w}$ between 5.5 and 5.7 S. This component represented 70%, 54% and 55% of the soluble protein for apoE2, apoE3 and apoE4, respectively. The sedimentation coefficients for the three most prominent structures, corrected for the density of the solvent and the solution viscosity, are given in Table 1. The diffusion coefficients determined from the sedimentation velocity data (Table 1) are in good agreement with those calculated from the R_S values. From the s and the D (calculated from Stokes radius) values, the molecular masses of each of the major species for the apolipoproteins in solution were calculated (Table 1). The three major species were characterized by molecular masses between 153.5 and 175.8 kDa, 69.3 and 81.9 kDa and 32.4 and 47.6 kDa, respectively. These analyses confirmed the presence of a 156-kDa tetramer as the major soluble species. The species with smaller s and R_S values possessed the molecular masses corresponding to dimers and monomers of recombinant apoE.

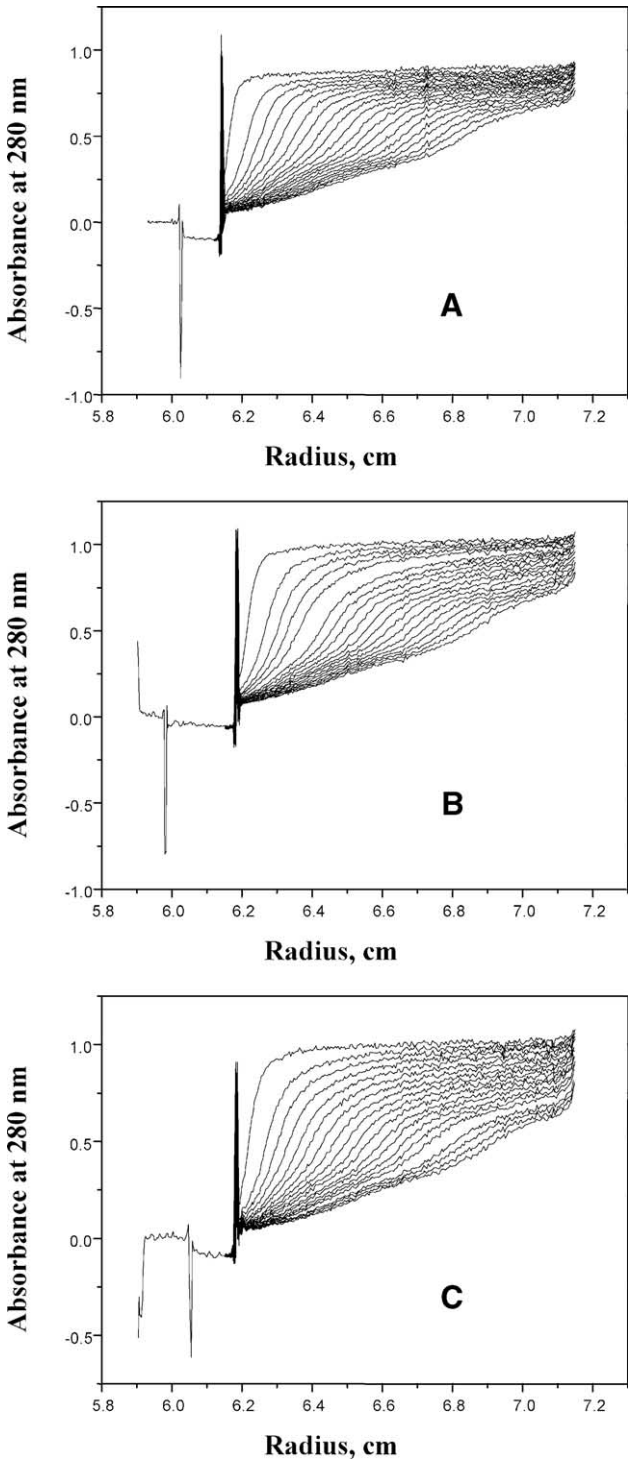

Fig. 2. Time-dependent mass distributions of the apoE isoforms upon analytical ultracentrifugation. Profiles were recorded during sedimentation velocity experiments at 60,000 rpm, 4 °C in 100 mM NH_4HCO_3 and 1 mM β-mercaptoethanol. (A) ApoE2, 0.35 mg/ml, (B) apoE3, 0.35 mg/ml, and (C) apoE4, 0.25 mg/ml.

3.3. Analysis of equilibrium sedimentation

To further analyze the self-association state of apolipoprotein E isoforms, equilibrium sedimentation analysis was performed (Fig. 4). The best fit of the experimental data corresponded to a monomer–dimer–tetramer equilibrium for apoE3, a monomer–dimer–tetramer–octamer equilibrium for apoE2 and a monomer–dimer–tetramer–octamer equilibrium for apoE4 (Fig. 4). The association constants for the self-association models are given in Table 2. The sedimentation equilibrium experiments revealed different self-association states for the recombinant apoE isoforms as compared to that of human plasma apoE3 which was found to exhibit a tetramer–octamer association at 0.5 mg/ml in aqueous solution. The apoE2 and apoE4 solutions contained some higher molecular weight structures that were larger than tetramers and that did not exist in apoE3 solutions. This conclusion is supported also by sedimentation velocity experiments (Fig. 3) whereas the gel filtration data were not as clear, probably, due to different $s(\sim M^{2/3})$ and $R_S(\sim M^{1/3})$ dependencies on molecular size [41] and a shift of the equilibrium to a less associated structure upon dilution of the protein during size exclusion chromatography. However, a deconvolution of the elution profiles into several Gaussians revealed the presence of at least one species intermediate in size between the aggregates and a tetrameric form.

Using the association constants reported in Table 2, the distributions of the oligomeric species were calculated

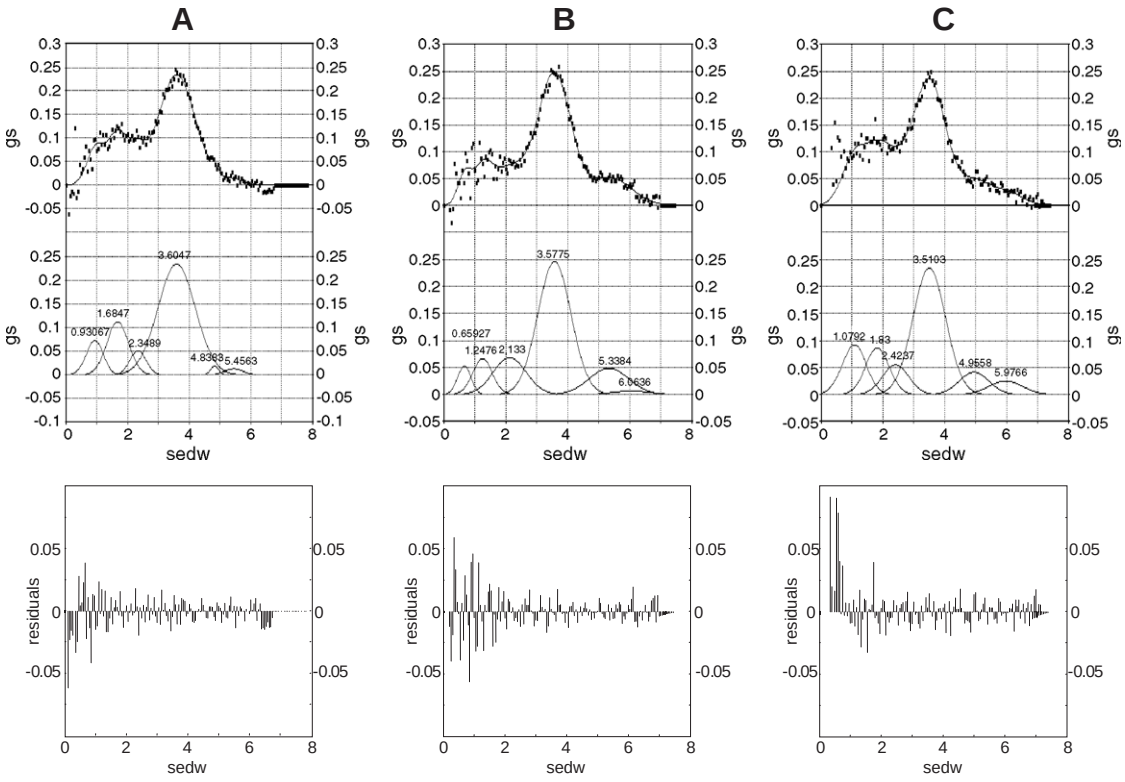

Fig. 3. Distribution of the species of the apoE isoforms in aqueous solution depending upon their sedimentation coefficient. (A) ApoE2, (B) apoE3, and (C) apoE4. Upper part, time derivative profile $g(s^*)$ and deconvolution with Gaussians. Lower part, residuals.

for the concentrations at which the gel filtration and the sedimentation velocity experiments were performed and these predicted values were compared with those observed experimentally. First and most important, the quantities of the oligomers predicted are in the range measurable by both the gel filtration and the sedimentation velocity techniques indicating that the models are reasonable. The models predict that tetramer and

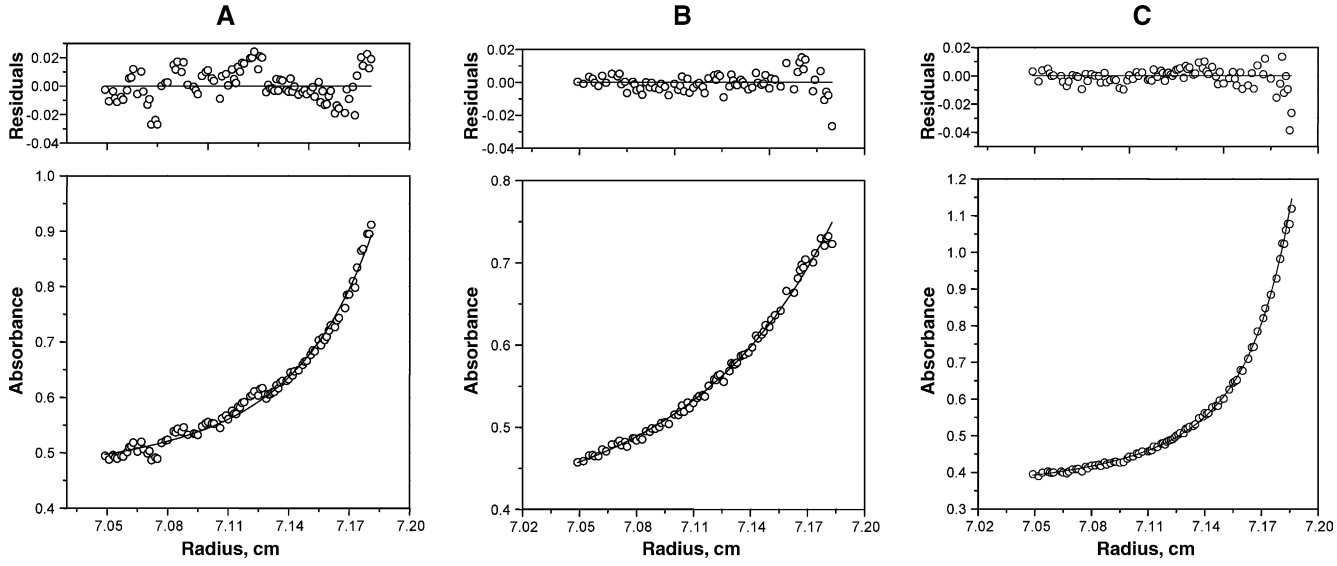

Fig. 4. Sedimentation equilibrium profiles and self-association schemes for the recombinant apoE isoforms. (A) For apoE2 at 10,000 rpm, the data were fitted to a monomer–dimer–tetramer–octamer association scheme; (B) for apoE3 at 10,000 rpm, a monomer–dimer–tetramer scheme was used; and (C) for apoE4 at 14000 rpm, a monomer–dimer–tetramer–octamer scheme was used. The association schemes were found to be similar at three sedimentation speeds (8000, 10000 and 14000 rpm). The concentrations of proteins dissolved in 100 mM NH_4HCO_3 and 1 mM DTT were 0.35 mg/ml for apoE2 and apoE3 and 0.25 mg/ml for apoE4. Upper part, residuals.

Table 2
Association constants for the modeling of apoE2, apoE3 and apoE4 self-association obtained from sedimentation equilibrium data

	$K_{1,2}$ (M^{-1})	$K_{1,4}$ (M^{-3})	$K_{1,8}$ (M^{-7})
apoE2	6.42×10^4	1.97×10^{16}	3.24×10^{38}
apoE3	2.66×10^5	6.69×10^{16}	–
apoE4	2.28×10^5	3.68×10^{17}	3.80×10^{40}

octamers should account for 65% and 71% of the apoE2 and apoE4 oligomers, respectively, in reasonable agreement with the 67% and 63% actually measured by sedimentation velocity. For gel filtration, the models predict 85% and 90% of the protein in the form of tetramers and octamers for apoE2 and apoE4, respectively, as compared to 70% and 71% actually measured. The decreased amounts measured could be related to the dilution. Monomers and dimers are predicted and measured to be less than 35% of the oligomeric species of apoE2 and apoE4. In contrast, monomers and dimers are predicted to represent 40–50% of apoE3 oligomers, in excellent agreement with the 44% observed by gel filtration. The measured value of about 25% measured by sedimentation velocity may be due to increased oligomerization during sedimentation. This discrepancy between the predicted and the measured amounts of monomers and dimers also exists for apoE2 and apoE4 but it is markedly less than in the case of apoE3 (approximately 32% predicted versus 23% measured).

3.4. Proteolysis study

The accessibility of the different proteases to their potential cleavage site(s) is determined by the tertiary structure of the protein that, in turn, may be influenced by the fusion peptide in this study. Five proteolytic enzymes with different specificities were used: trypsin (arginine and lysine), chymotrypsin (tyrosine, phenylalanine, tryptophane and leucine), elastase (alanine and valine), subtilisin (non-specific residue, but charged amino acids preferred) and *Staphylococcus aureus* V8 protease (glutamic acid) [43]. All five enzymes produced stable intermediates upon proteolysis of plasma apoE3 [11]. The formation of stable intermediates composed of two groups of fragments was observed upon proteolysis of the recombinant apoE isoforms (Fig. 5). The first group appeared to be composed of fragments corresponding to an amino-terminal domain; this judgement was based upon apparent molecular masses between 38 and 20 kDa and the interaction with either the 3B7 or 1D7 anti-apoE monoclonal antibody (Table 3). The second group included fragments with apparent molecular masses less than 16 kDa that interacted with the 3H1 anti-apoE monoclonal antibody thus indicating that these fragments were part or all of CT domain (Table 3). The presence of the fusion peptide thus seems not to change the tertiary organization of apolipoprotein E.

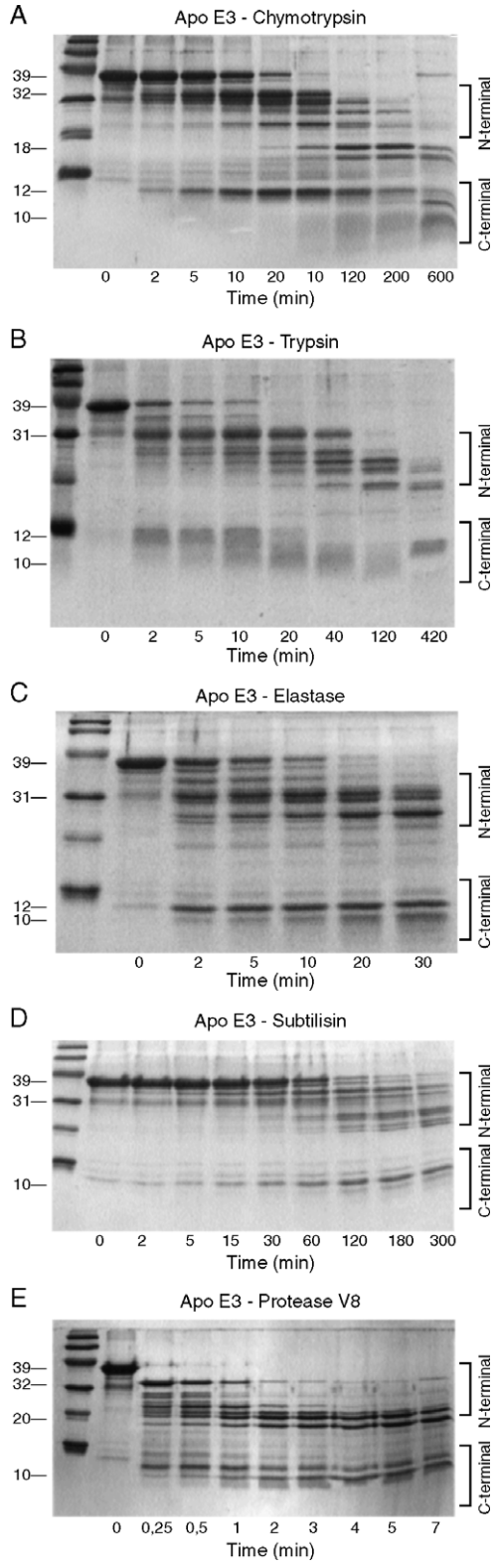

Fig. 5. Time course of recombinant apoE3 limited proteolysis by various proteolytic enzymes as assessed by SDS-PAGE on a 15–20% gradient polyacrylamide gel. Molecular weight markers on the first lane corresponded to 94-66-43-30-20.1-14.4 kDa. Arrows indicate molecular masses of some fragments. Limited proteolysis by (A) chymotrypsin (enzyme-to-substrate ratio E:S=1:200, *w*/*w*); (B) trypsin (E:S=1:2000, *w*/*w*); (C) elastase (E:S=1:150, *w*/*w*); (D) subtilisin (E:S=1:5000, *w*/*w*); and (E) *S. aureus* V8 protease (E:S=1:30, *w*/*w*).

Table 3
Summary of fragment analysis from limited proteolysis of recombinant apoE3

	Molecular mass, kDa	Monoclonal antibody reactivity			Probable identification
		3B7	1D7	3H1	
Trypsin	36.0	+	+	+	24–342
	30.5	+	+	+	45–317
	28.5	+	+	–	3–249
	27.5	+	+	–	3–234
	26.0	+	+	–	3–223
	23.5	ND	ND	ND	24–223; 45–249
	19.0	ND	ND	ND	45–223
	13.0	–	–	+	234–342
	11.0	–	–	+	268–342
Chymotrypsin	38.0				27–342
	32.0				64–342
	30.0				1–257; 64–319
	26.3				27–257
	23.0				1–198; 64–257
	17.8				64–217
	16.1				64–198
	11.8				242–342
	10.8				247–342
	8.9				258–342
Elastase	38.0	+	+	+	14–342
	34.0	+	+	+	40–342
	31.0	+	+	–	1–259
	30.0	+	+	–	1–242
	26.0	+	+	–	14–236
	25.0	ND	ND	ND	39–259
	23.0	ND	ND	ND	46–236
	20.0	ND	ND	ND	46–218
	12.5	–	–	+	236–342
	11.5	–	–	+	259–342
Subtilisin	37.5				17–342
	34.5				42–342
	31.0				1–255
	25.5				17–237; 42–262
	24.4				17–230; 42–255
	22.2				42–237; 62–255
	20.7				
	13.7				
	12.1				238–342
	11.0				249–342
S. aureus V8	34.0				47–342
	28.0				1–248
	27.0				1–229
	24.0				56–262
	23.1				56–248
	21.0				56–229
	20.3				56–222
	18.2				56–211; 63–222
	11.2				249–342
	9.5				263–342

Compared to the plasma apoE3 digestion profile, the number and the apparent size of carboxyl-terminal fragments obtained with the recombinant apoE3 were the same, which suggest similarly located cleavage sites in the proteins. On the other hand, the number of amino-terminal fragments obtained with the recombinant apoE3 isoform was greater than that obtained with plasma apoE3. Also some of the amino-terminal fragments possessed an apparent molecular mass greater than those obtained for plasma apoE3 apparently due to the presence of the fusion peptide. Proteolysis of the hinge region appeared to occur before cleavage of sites within the fusion peptide. A 30-kDa fragment appeared during proteolysis with trypsin and elastase, which was recognized by all three monoclonal anti-apoE antibodies (Table 3). Its size and immunoreactivity suggested that an accessible cleavage site was located in the region 273–278. Based upon results with nuclear magnetic resonance this region is believed to form a bend [44]. This region was not accessible in the plasma apoE3. All amino-terminal fragments of the plasma apoE3 had carboxyl-terminal extremities located in the hinge region 167–210 [11]. The digestion profiles of recombinant apoE2 and apoE4 were very similar to that of recombinant apoE3 and included two groups of stable fragments. The first group consisted of fragments with apparent molecular masses between 38 and 20 kDa that interacted at least with either the 3B7 or the 1D7 monoclonal antibody. The second group contained fragments with apparent molecular masses smaller than 16 kDa that were recognized by the 3H1 antibody. The accessible cleavage sites of all five proteolytic enzymes in recombinant apoE2 were identical to those in recombinant apoE3. The principal sites were located in the hinge region and in the fusion peptide. The bend in the carboxyl domain (273–278 region) was also accessible in the recombinant apoE2.

The amino-terminal fragments of the recombinant apoE4 isoform were very similar in size and in number to those obtained with the other apoE isoforms suggesting that similar cleavage sites were accessible in this part of the protein molecule. However, both the number and the apparent molecular masses of the carboxyl-terminal fragments differed from those of recombinant apoE2 or apoE3. Depending on the enzyme, one or four fragments appeared with apparent molecular masses in the range of 16 to 10 kDa (Table 4). The localization of these fragments was deduced from the apparent molecular masses. 16 or 14 kDa fragments appeared initially which were subsequently degraded to fragments with molecular masses of 12 to 10 kDa. The region from residue 202 to 224 was cleaved initially and then the region between the residues 230 and 260 was attacked. In contrast, in the apoE3 or the apoE2 isoforms this second 230–260 region was preferentially cleaved and the 16 or the 14 kDa carboxyl-terminal fragments did not appear. It appears that this region in the apoE4 molecule, as compared to apoE3 and apoE2, was not

Table 4
Analysis of carboxyl-terminal fragments in limited proteolysis of recombinant apoE4

	Molecular mass, kDa	Probable identification
Trypsin	15	210 or 214–342
	12	234–342
	10	250–342
Chymotrypsin	14	217 or 224–342
	12	242–342
	10	258–342
Elastase	16	202–342
	15	212–342
	14	218–342
	10	259–342
Subtilisin	14	223–342
	12	238–342
S. aureus V8	16	211–342
	14	222 or 229–342
	12	249–342
	10	263–342

easily accessible to different proteolytic enzymes, i.e. it was protected or stabilized.

4. Discussion

4.1. Self-association

The association states of three recombinant apoE isoforms were analyzed by three different techniques that allowed, firstly, to establish the role of the NT domain of apoE and, secondly, to compare the association states of the recombinant apoE isoforms with each other and to human plasma apoE3.

The self-association of all three recombinant apoE isoforms was different from that of plasma apoE3. Both by gel filtration and by sedimentation velocity, plasma apoE3 seemed to exist mainly as tetramer whereas all three recombinant apolipoproteins displayed additional heterogeneity. A tetramer for plasma apoE of unspecified phenotype [19], a tetramer–octamer association for plasma apoE3 [10] and a more complex association scheme that included native and partially denatured tetramer and monomer for the plasma apolipoprotein [27,28] have been previously described. However, the recombinant apoE isoforms in our study presented more complex association schemes that included octamer, tetramer, dimer and monomer. The different temperatures used in these studies do not seem to contribute significantly to the different self-association schemes of plasma and recombinant apolipoproteins. The presence of smaller species in the association schemes in the current study seemed to be a characteristic feature of the recombinant apoE isoforms, which contain an amino-terminal extension of 43 amino acids. In another study with recombinant apoE3 and apoE4, dimers were not observed and the authors suggested the existence of a slow equilibrium between monomer, tetramer and octamer, with apoE4 being more associated [29]. However, the N-terminal-truncated apoE3 (72–299) existed as a major species with a *s* value of 5.9 S, apoE4 (72–299) showed a wider and more complicated species distribution [30]. The addition of a fused peptide in the NT domain appears to induce some changes in the properties of the carboxyl-terminal domain. The two compact apoE structural domains are separated by a hinge region but some interactions may exist between them [22]. The presence of the fused peptide in the NT domain could disturb the interactions between N- and C-terminal domains. Indeed, it has been shown that a Glu3→Lys mutation induced an increased affinity for the LDL receptor [12,16]. Although this residue is localized within a non-structured region (the first α-helix consists of Gln24 to Thr42), it is very important in LDL-receptor binding. However, the major structural and functional features found in plasma apoE3 seem to be conserved in the recombinant apolipoproteins. For example: (1) the apoE3 and apoE4 recombinant apoE isoforms possessed LDL-receptor binding activity similar to that of plasma apoE3 [33], whereas apoE2 did not bind; (2) the presence of the fused peptide did not induce a greater sensitivity to proteases within either the C- or N-terminal domains, reflecting the integrity of a compact structure for these domains; and (3) the fused peptide did not drastically reduce the immunoreactivity of the CT domain-specific antibody 3H1 toward the epitope within the 243–272 region [33]. Also, the additional uncleaved or residual N-terminal sequence of variable length did not influence the functional and structural properties of recombinant apoA-I [45] and apoE [46]. The self-association of plasma apoE has been shown to be a property of the CT domain, the amino-terminal domain remaining monomeric even at high protein concentrations [10]. The tetramer formation mediated by the CT domain was suggested to proceed through a four-helix bundle [10] or an intermolecular coiled-coil [31] where the tetramer may be modeled as a dimer of dimers with a parallel or an anti-parallel alignment. The segment that bears a propensity to form coiled-coil helices in the CT domain is composed of residues 218–266 and coincides with the putative lipoprotein-binding sequence. A coiled-coil homodimer upon juxtaposition with a neighboring dimer could promote formation of a four-helix bundle via residues 267–299 [31]. It should be noted that a possibility for coiled-coil formation in the NT domain was also suggested by these authors. The observation of a dimer in our study supports the contribution of a coiled-coil structure in apoE self-association.

ApoE polymorphisms clearly influence the self-association of the apolipoprotein in aqueous solutions. As assessed by size exclusion liquid chromatography, apoE2 and apoE4 are predominantly composed of tetramers (65% of the total soluble species), whereas recombinant apoE3 showed one monomeric, 4.0-nm species that represented 50% of the soluble species. This tendency of apoE2 and apoE4 to self-associate as high-molecular weight oligomers

has been confirmed also by sedimentation equilibrium analysis. The association schemes for apoE2 and apoE4 included octameric species, while the equilibrium distribution of apoE3 was fitted well by a monomer–dimer–tetramer association scheme. By sedimentation velocity analysis, the three proteins presented a major soluble species with a sedimentation coefficient between 5.5 and 5.6 S, corresponding to tetramers. However, higher molecular mass oligomers with the *s* values as 7.6–8.4 S and 8.6–9.4 S were also evident by $g(s^*)$ analysis and their size and content varied between three isoforms. The differences between apoE2 and apoE4 on the one hand and apoE3 on the other were supported by the good general agreement between the calculated (from the association constants determined by sedimentation equilibrium) and the measured (gel filtration and sedimentation velocity) amounts of tetrameric and larger species. However, the amount of monomer measured by sedimentation velocity was less than predicted for all the isoforms. The isoforms differed however in that this difference was more marked in the case of apoE3 than for apoE2/E4. An uncoupling, on the time scale of the sedimentation, of the rapidly sedimenting oligomers from the slower sedimenting components [29] might partially explain this difference.

4.2. Domain organization

The existence of two domains seems to be a characteristic feature of the structure of exchangeable apolipoproteins such as apoA-I and apoE [47]. The analysis of the domain organization within the three recombinant apoE isoforms was studied by limited proteolysis. The fusion peptide did not influence the CT domain whereas it had an effect on the NT domain. Proteolysis within the fusion peptide began after the cleavage of the hinge region, extending the available sites compared to the profile described for plasma apoE3 [11] although the basic domain structure was preserved. In all three recombinant isoforms digested by trypsin and elastase, a cleavable site, not accessible in plasma apolipoprotein E3 and in addition to the hinge region 167–210 [11], was revealed in the region 273–278 which forms a bend in plasma apoE3. A specific organization of the apoE4 CT domain was found. The presence of stable 16–14 kDa C-terminal fragments that did not exist in the two other isoforms suggested a different tertiary structure of the CT domain in apoE4 as compared to apoE2 and apoE3. The NT domains of the three apoE isoforms have been crystallized [20]. However, crystallographic data on the CT domains or the whole apoproteins are lacking. The presence of a positive charge at position 112 in apoE4 compared to apoE3 due to the cysteine–arginine interchange could create a salt bridge with the glutamic acid residue at position 109, which does not exist in other isoforms. This salt bridge in apoE4 results in a more exterior location of the side chain of Arg61 adjacent to residue 112 [20]. This arginine 61 has been shown to be a critical residue in the different distributions of the various apoE isoforms among lipoproteins [21] due to the interaction with glutamic acid 255 in CT domain [22]. This interaction may stabilize an extended helical structure in the CT domain and induce the preferential binding of apoE4 to VLDL. Segrest et al. have suggested that the length of the amphiphatic α-helix is an important determinant of lipoprotein association [48]. Arginine 61 does not interact with glutamic acid 255 in apoE3 or apoE2 and, in these cases, the shorter helix would bind preferentially to HDL. Our results seem to confirm the higher stability of the region in the vicinity of glutamic acid 255 in apoE4 since 230–260 region was protease-resistant in apoE4 but not in apoE3 or apoE2. These results confirm the domain interaction in apoE4. Other studies, however, suggest that this interaction exists only in lipid-bound state of this isoform [23].

In conclusion, we have shown here novel apoE isoform-specific self-association schemes and interdomain interactions. The secondary and tertiary structures of the three recombinant isoforms are analysed in more detail in a paper that follows [49].

Acknowledgements

This work was supported in part by the Centre National de la Recherche Scientifique (C.N.R.S.), the Institut National de la Santé et de la Recherche Médicale (I.N.S.E.R.M.), the Caisse Nationale de l'Assurance Maladie des Travailleurs Salariés (C.N.A.M.T.S.), the Ministère de l'Enseignement Supérieur et de la Recherche, the Fondation Pour la Recherche Médicale and the European Economic Community (contract MAT1-CT94046). A.D.D. thanks the Russian Foundation for Basic Research for financial support, grant 04-04-48165.

References

[1] M.S. Brown, J.L. Goldstein, A receptor-mediated pathway for cholesterol homeostasis, Science 232 (1986) 34–47.
[2] J. Herz, U. Hamann, S. Rogne, O. Myklebost, H. Gausepohl, K.K. Stanley, Surface location and high affinity for calcium of a 500-kd liver membrane protein closely related to the LDL-receptor suggest a physiological role as lipoprotein receptor, EMBO J. 7 (1988) 4119–4127.
[3] G. Utermann, M. Jaeschke, J. Menzel, Familial hyperlipoproteinemia type III: deficiency of a specific apolipoprotein (apo E-III) in the very-low-density lipoproteins, FEBS Lett. 56 (1975) 352–355.
[4] K.H. Weisgraber, Apolipoprotein E: structure–function relationships, Adv. Protein Chem. 45 (1994) 249–302.
[5] E.H. Corder, A.M. Saunders, W.J. Strittmatter, D.E. Schmechel, P.C. Gaskell, G.W. Small, A.D. Roses, J.L. Haines, M.A. Pericak-Vance, Gene dose of apolipoprotein E type 4 allele and the risk of Alzheimer's disease in late onset families, Science 261 (1993) 921–923.
[6] A. Steinmetz, C. Jakobs, S. Motzny, H. Kaffarnik, Differential distribution of apolipoprotein E isoforms in human plasma lipoproteins, Arteriosclerosis 9 (1989) 405–411.

[7] W.J. Strittmatter, K.H. Weisgraber, D.Y. Huang, L.M. Dong, G.S. Salvesen, M. Pericak-Vance, D. Schmechel, A.M. Saunders, D. Goldgaber, A.D. Roses, Binding of human apolipoprotein E to synthetic amyloid beta peptide: isoform-specific effects and implications for late-onset Alzheimer disease, Proc. Natl. Acad. Sci. U. S. A. 90 (1993) 8098–8102.
[8] K.H. Weisgraber, T.L. Innerarity, R.W. Mahley, Abnormal lipoprotein receptor-binding activity of the human E apoprotein due to cysteine–arginine interchange at a single site, J. Biol. Chem. 257 (1982) 2518–2521.
[9] R.E. Pitas, Microtubule formation and neurite extension are blocked by apolipoprotein E4, Cell Dev. Biol. Eye 7 (1996) 725–731.
[10] L.P. Aggerbeck, J.R. Wetterau, K.H. Weisgraber, C.S. Wu, F.T. Lindgren, Human apolipoprotein E3 in aqueous solution: II. Properties of the amino- and carboxyl-terminal domains, J. Biol. Chem. 263 (1988) 6249–6258.
[11] J.R. Wetterau, L.P. Aggerbeck, S.C. Rall Jr., K.H. Weisgraber, Human apolipoprotein E3 in aqueous solution: I. Evidence for two structural domains, J. Biol. Chem. 263 (1988) 6240–6248.
[12] L.M. Dong, T. Yamamura, S. Tajima, A. Yamamoto, Site-directed mutagenesis of an apolipoprotein E mutant, apo E5(Glu3→Lys) and its binding to low density lipoprotein receptors, Biochem. Biophys. Res. Commun. 187 (1992) 1180–1186.
[13] Y. Horie, S. Fazio, J.R. Westerlund, K.H. Weisgraber, S.C. Rall Jr., The functional characteristics of a human apolipoprotein E variant (cysteine at residue 142) may explain its association with dominant expression of type III hyperlipoproteinemia, J. Biol. Chem. 267 (1992) 1962–1968.
[14] A. Lalazar, K.H. Weisgraber, S.C. Rall Jr., H. Giladi, T.L. Innerarity, A.Z. Levanon, J.K. Boyles, B. Amit, M. Gorecki, R.W. Mahley, Site-specific mutagenesis of human apolipoprotein E. Receptor binding activity of variants with single amino acid substitutions, J. Biol. Chem. 263 (1988) 3542–3545.
[15] M.R. Wardell, K.H. Weisgraber, L.M. Havekes, S.C. Rall Jr., Apolipoprotein E3-Leiden contains a seven-amino acid insertion that is a tandem repeat of residues 121–127, J. Biol. Chem. 264 (1989) 21205–21210.
[16] M.R. Wardell, S.C. Rall Jr., E.J. Schaefer, J.P. Kane, K.H. Weisgraber, Two apolipoprotein E5 variants illustrate the importance of the position of additional positive charge on receptor-binding activity, J. Lipid Res. 32 (1991) 521–528.
[17] C. Wilson, T. Mau, K.H. Weisgraber, M.R. Wardell, R.W. Mahley, D.A. Agard, Salt bridge relay triggers defective LDL receptor binding by a mutant apolipoprotein, Structure 2 (1994) 713–718.
[18] K.H. Weisgraber, S.C. Rall Jr., R.W. Mahley, R.W. Milne, Y.L. Marcel, J.T. Sparrow, Human apolipoprotein E. Determination of the heparin binding sites of apolipoprotein E3, J. Biol. Chem. 261 (1986) 2068–2076.
[19] S. Yokoyama, Y. Kawai, S. Tajima, A. Yamamoto, Behavior of human apolipoprotein E in aqueous solutions and at interfaces, J. Biol. Chem. 260 (1985) 16375–16382.
[20] M.R. Wardell, C. Wilson, D.A. Agard, R.W. Mahley, K.H. Weisgraber, in: C.R. Sirtori, G. Franceschini, H.B. Brewer Jr. (Eds.), Crystal Structures of the Common Apolipoprotein E Variants: Insights into Functional Mechanisms, NATO ASI Series, vol. II 73, Springer-Verlag, Berlin, 1993, pp. 81–96.
[21] L.M. Dong, C. Wilson, M.R. Wardell, T. Simmons, R.W. Mahley, K.H. Weisgraber, D.A. Agard, Human apolipoprotein E. Role of arginine 61 in mediating the lipoprotein preferences of the E3 and E4 isoforms, J. Biol. Chem. 269 (1994) 22358–22365.
[22] L.M. Dong, K.H. Weisgraber, Human apolipoprotein E4 domain interaction. Arginine 61 and glutamic acid 255 interact to direct the preference for very low density lipoproteins, J. Biol. Chem. 271 (1996) 19053–19057.
[23] J.A. Morrow, M.L. Segall, S. Lund-Katz, M.C. Phillips, M. Knapp, B. Rupp, K.H. Weisgraber, Differences in stability among the human apolipoprotein E isoforms determined by the amino-terminal domain, Biochemistry 39 (2000) 11657–11666.
[24] P. Acharya, M.L. Segall, M. Zaiou, J. Morrow, K.H. Weisgraber, M.C. Phillips, S. Lund-Katz, J. Snow, Comparison of the stabilities and unfolding pathways of human apolipoprotein E isoforms by differential scanning calorimetry and circular dichroism, Biochim. Biophys. Acta 1584 (2002) 9–19.
[25] M. Forstner, C. Peters-Libeu, E. Contreras-Forrest, Y. Newhouse, M. Knapp, B. Rupp, K.H. Weisgraber, Carboxyl-terminal domain of human apolipoprotein E: expression, purification, and crystallization, Protein Expr. Purif. 17 (1999) 267–272.
[26] J. Dong, M.E. Balestra, Y.M. Newhouse, K.H. Weisgraber, Human apolipoprotein E7: lysine mutations in the carboxy-terminal domain are directly responsible for preferential binding to very low-density lipoproteins, J. Lipid Res. 41 (2000) 1783–1789.
[27] A.D. Dergunov, V.V. Shuvaev, E.V. Yanushevskaja, Quaternary structure of apolipoprotein E in solution: fluorimetric, chromatographic and immunochemical studies, Biol. Chem. Hoppe-Seyler 373 (1992) 323–331.
[28] A.D. Dergunov, Y.Y. Vorotnikova, S. Visvikis, G. Siest, Homo- and hetero-complexes of exchangeable apolipoproteins in solution and in lipid-bound form, Spectrochim. Acta, Part A 59 (2003) 1127–1137.
[29] M. Perugini, P. Schuck, G.J. Howlett, Self-association of human apolipoprotein E3 and E4 in the presence and absence of phospholipid, J. Biol. Chem. 275 (2000) 36758–36765.
[30] C.Y. Chou, Y.L. Lin, Y.C. Huang, S.Y. Sheu, T.H. Lin, H.J. Tsay, G.G. Chang, M.S. Shiao, Structural variation in human apolipoprotein E3 and E4: secondary structure, tertiary structure, and size distribution, Biophys. J. 88 (2005) 455–466.
[31] N. Choy, V. Raussens, V. Narayanaswami, Inter-molecular coiled-coil formation in human apolipoprotein E C-terminal domain, J. Mol. Biol. 334 (2003) 527–539.
[32] K.H. Weisgraber, S.C. Rall Jr., R.W. Mahley, Human E apoprotein heterogeneity. Cysteine–arginine interchanges in the amino acid sequence of the apo-E isoforms, J. Biol. Chem. 256 (1981) 9077–9083.
[33] A. Barbier, A. Visvikis, F. Mathieu, L. Diez, L.M. Havekes, G. Siest, Characterization of three human apolipoprotein E isoforms (E2, E3 and E4) expressed in *Escherichia coli*, Eur. J. Clin. Chem. Clin. Biochem. 35 (1997) 581–589.
[34] T. Pillot, A. Barbier, A. Visvikis, K. Lozac'h, M. Rosseneu, J. Vandekerckhove, G. Siest, Single-step purification of two functional human apolipoprotein E variants hyperexpressed in *Escherichia coli*, Protein Expr. Purif. 7 (1996) 407–414.
[35] H.J. Pownall, J.B. Massey, Spectroscopic studies of lipoproteins, Methods Enzymol. 128 (1986) 515–518.
[36] M. Le Maire, A. Ghazi, J.V. Moller, L.P. Aggerbeck, The use of gel chromatography for the determination of sizes and relative molecular masses of proteins. Interpretation of calibration curves in terms of gel-pore-size distribution, Biochem. J. 243 (1987) 399–404.
[37] V.N. Uversky, Use of fast protein size-exclusion liquid chromatography to study the unfolding of proteins which denature through the molten globule, Biochemistry 32 (1993) 13288–13298.
[38] W.F. Stafford, Boundary analysis in sedimentation transport experiments: a procedure for obtaining sedimentation coefficient distributions using the time derivative of the concentration profile, Anal. Biochem. 203 (1992) 295–301.
[39] J.S. Philo, A method for directly fitting the time derivative of sedimentation velocity data and an alternative algorithm for calculating sedimentation coefficient distribution functions, Anal. Biochem. 279 (2000) 151–163.
[40] T. Laue, Biophysical studies by ultracentrifugation, Curr. Opin. Struct. Biol. 11 (2001) 579–583.
[41] J. Lebowitz, M.S. Lewis, P. Schuck, Modern analytical ultracentrifugation in protein science: a tutorial review, Protein Sci. 11 (2002) 2067–2079.

[42] R.W. Milne, P. Douste-Blazy, Y.L. Marcel, L. Retegui, Characterization of monoclonal antibodies against human apolipoprotein E, J. Clin. Invest. 68 (1981) 111–117.
[43] J.S. Bond, Proteolytic enzymes: a practical approach, eds R.J. Beynon and J. S. Bond (IRL Press, Oxford University Press, 1989).
[44] G. Wang, G.K. Pierens, W.D. Treleaven, J.T. Sparrow, R.J. Cushley, Conformations of human apolipoprotein E(263–286) and E(267–289) in aqueous solutions of sodium dodecyl sulfate by CD and ^{1}H NMR, Biochemistry 35 (1996) 10358–10366.
[45] J. Bergeron, P.G. Frank, F. Emmanuel, M. Latta, Y. Zhao, D.L. Sparks, E. Rassart, P. Denefle, Y.L. Marcel, Characterization of human apolipoprotein A-I expressed in *Escherichia coli*, Biochim. Biophys. Acta 1344 (1997) 139–152.
[46] J.A. Morrow, K.S. Arnold, K.H. Weisgraber, Functional characterization of apolipoprotein E isoforms overexpressed in *Escherichia coli*, Protein Expr. Purif. 16 (1999) 224–230.
[47] H. Saito, P. Dhanasekaran, D. Nguyen, P. Holvoet, S. Lund-Katz, M.C. Phillips, Domain structure and lipid interaction in human apolipoproteins A-I and E, a general model, J. Biol. Chem. 278 (2003) 23227–23232.
[48] J.P. Segrest, M.K. Jones, H. De Loof, C.G. Brouillette, Y.V. Venkatachalapathi, G.M. Anantharamaiah, The amphipathic helix in the exchangeable apolipoproteins: a review of secondary structure and function, J. Lipid Res. 33 (1992) 141–166.
[49] V. Clement-Collin, A. Barbier, A.D. Dergunov, A. Visvikis, G. Siest, M. Desmadril, M. Takahashi, L.P. Aggerbeck, The structure of human apolipoprotein E2, E3 and E4 in solution: 2. Multidomain organiza tion correlates with the stability of apoE structure, Biophys. Chemist. 119 (2005—this issue) 158–173, doi:10.1016/j.bpc.2005.07.009.